Volume Title
*ASP Conference Series, Vol. **Volume Number***
Author
© ***Copyright Year** Astronomical Society of the Pacific*

arXiv:1108.4051v1 [astro-ph.SR] 19 Aug 2011

Fundamental Properties of Young Binary Stars

Gail H. Schaefer[1]

[1]*The CHARA Array of Georgia State University, Mount Wilson Observatory, Mount Wilson, CA 91023*

Abstract. Spatially resolving the orbits of double-lined spectroscopic binaries provides a way to measure the dynamical masses of the component stars. At the distances to the nearest star forming regions, high angular resolution techniques are required to resolve these short period systems. In this paper, I provide an overview of the few low-mass pre-main-sequence spectroscopic binaries that have been resolved thus far using long-baseline optical/infrared interferometers. I also compiled a list of known spectroscopic binaries in nearby star forming regions (Taurus, Orion, Ophiuchus, Scorpius-Centaurus, etc.) and show that with modest improvements in the sensitivity of interferometers with 200-300 meter baselines, we can build a significant set of pre-main sequence stars with precise mass determinations. This is important for validating and distinguishing among the theoretical calculations of evolution for young stars.

1. Introduction

Determining precise masses and ages of pre-main-sequence (PMS) stars is important for understanding how stars form and evolve over time. Different theoretical models of stellar evolution predict a large range of stellar masses for a given effective temperature, luminosity, and metallicity at young ages. This is particularly the case for low-mass PMS stars ($M < 1\ M_{\odot}$; e.g. Simon 2001; Hillenbrand & White 2004; Mathieu et al. 2007). Discrepancies between the models arise from differences in the treatment of interior convection, atmospheric opacities, and initial conditions (e.g. Allard et al. 1997; Chabrier & Baraffe 2000; Baraffe et al. 2003). Figure 1 illustrates the discrepancies among different evolutionary models. Measuring precise masses of young stars is required for testing the different sets of evolutionary tracks.

Stellar masses can be measured through the following dynamical techniques: (1) observations of eclipsing double-lined spectroscopic binaries where the masses and radii of the component stars are determined from the radial velocity variations and timing of the eclipse light curve (Torres summarized results from eclipsing binaries at this conference), (2) spatially resolving the visual orbit of a double-lined spectroscopic binary to determine the component stellar masses and distance to the system, (3) measuring the astrometric motion of component stars around their center of mass (e.g. the triple system Elias 12; Schaefer et al. 2010), (4) mapping the Keplerian rotation of circumstellar disks to determine the mass of the central star (Guilloteau & Dutrey 1998; Simon et al. 2000). The last two techniques require an accurate parallax to scale the masses to the proper distance. Figure 2 shows a histogram of the current sample of dynamical masses of PMS stars measured using these techniques.

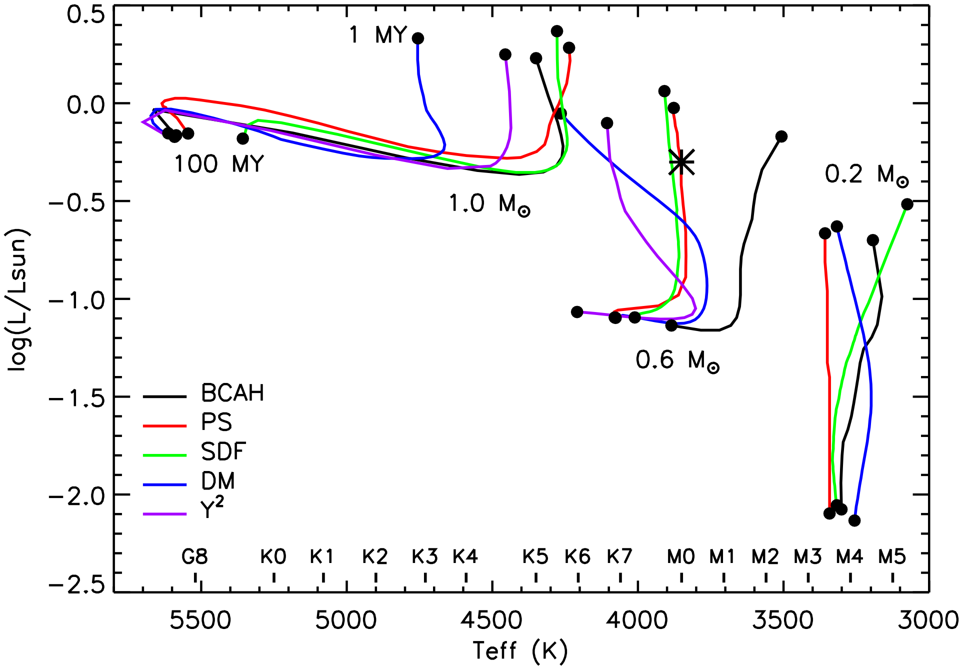

Figure 1. Pre-main-sequence evolutionary tracks computed by D'Antona & Mazzitelli (1997, DM), Baraffe et al. (1998, BCAH), Palla & Stahler (1999, PS), Siess et al. (2000, SDF), and Yi et al. (2003, Y^2). The tracks are for masses of 0.2, 0.6, and 1.0 $M_\odot$ and correspond to ages from 1 Myr to 100 Myr. We indicate spectral types based on the effective temperature relations used in Kenyon & Hartmann (1995) for G8-M0 and the T-Tauri temperature scale defined in Luhman et al. (2003) for M1-M7. The asterisk shows the location of an M0 star with 0.5 $L_\odot$.

In this paper I focus on spatially resolving double-lined spectroscopic binaries to determine the masses of PMS stars. In addition to masses, a comparison of the physical size of the projected semi-major axis from the spectroscopic orbit ($a \sin i$ in AU) with the angular scale (a in mas) and inclination i from the visual orbit provide an orbital parallax for the system. Accurate distances are necessary for determining the absolute magnitudes and luminosities for plotting the stars on the HR diagram to compare with evolutionary tracks. Additionally, distances for independent systems will aid in mapping the three-dimensional structure of nearby star-forming regions (Loinard et al. 2008; Torres et al. 2009). The distribution of masses, mass ratios, and orbital parameters of PMS binaries across a variety of star forming regions will help test theories of binary star formation (Ballesteros-Paredes et al. 2007; Bonnell et al. 2007).

2. Interferometric Observations of Young Binary Stars

Double-lined spectroscopic binaries tend to sample short-period systems ($P < 10$ years, corresponding to velocity amplitudes $< 5-10$ km/s). For a circular binary with equal mass components and a total mass of 1 $M_\odot$, a period of 10 years corresponds to a

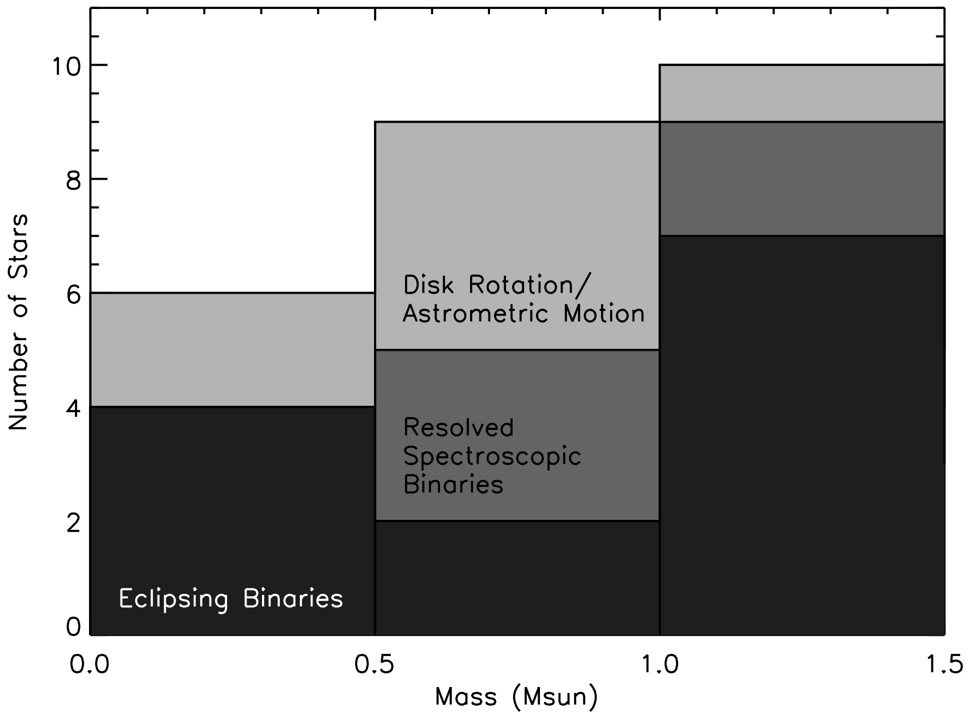

Figure 2. Histogram of dynamical mass measurements of low-mass stars in nearby star forming regions (Taurus, Orion, Ophiuchus, Scorpius-Centaurus, TW Hydra) with internal precision measured to better than ~ 10%. The shaded bins indicate the method of mass measurement: eclipsing spectroscopic binaries (black), spatially resolved spectroscopic binaries (dark grey), and Keplerian rotation of circumstellar disks and astrometric center of mass motion in visual binaries (light grey). Note that the masses in the last category are dependent on the distance to the star. References for eclipsing SB: Popper (1987), Alencar et al. (2003), Covino et al. (2004), Stassun et al. (2004), Irwin et al. (2007), Cargile et al. (2008), Stempels et al. (2008); resolved SB: Steffen et al. (2001), Boden et al. (2005); disk rotation: Simon et al. (2000), Prato et al. (2002); and astromery: Schaefer et al. (2010).

.

semi-major axis of 4.6 AU or ~ 33 mas for an edge-on system scaled to the distance of the Taurus star forming region ($d \sim 140$ pc). The diffraction limit ($1.22\lambda/D$) of a 10-meter telescope in the H-band is ~ 40 mas. Therefore, binaries that can be spatially resolved through adaptive optics imaging, speckle interferometry, or aperture masking using large aperture telescopes in the infrared or with the Hubble Space Telescope in the optical have periods measured on the order of decades or longer (e.g. Schaefer et al. 2006). Clearly, long-baseline optical/infrared interferometry is required to spatially resolve the short period spectroscopic binaries in nearby star-forming regions.

The PMS double-lined spectroscopic binary NTT 045251+3016 was spatially resolved using the Fine Guidance Sensors on the Hubble Space Telescope by Steffen et al. (2001). At smaller separations, long-baseline interferometry becomes a critical tool for resolving young binary systems. Interferometers measure the fringe contrast or visibil-

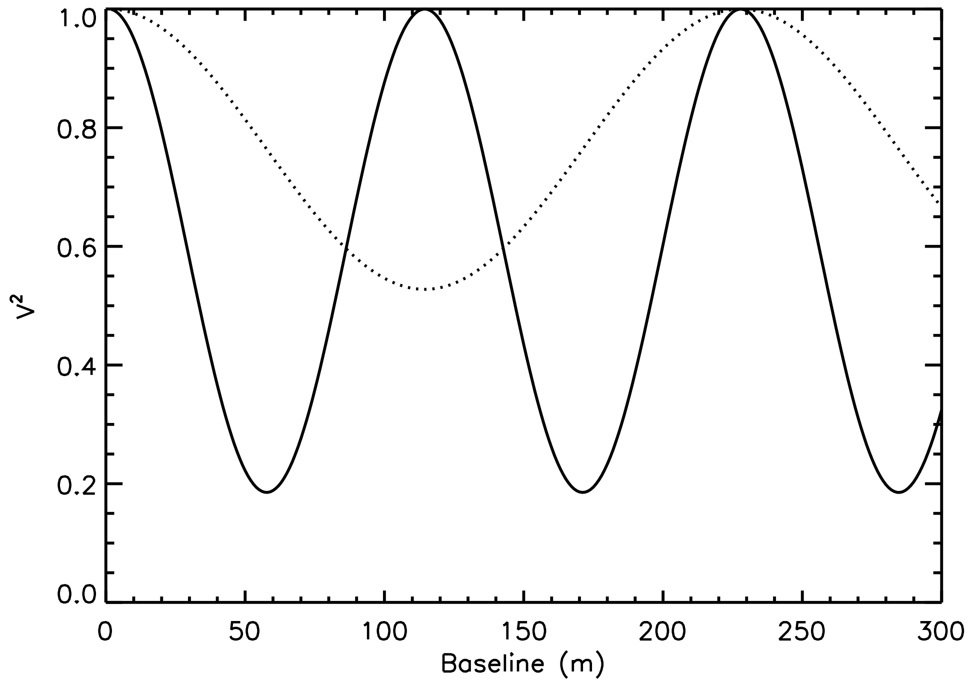

Figure 3. Example visibility curves of a binary star in the K-band for interferometer baselines out to 300 meters. The solid line shows a 4.0 mas binary system with a flux of $\Delta K = 1.0$, while the dotted line shows a 2.0 mas binary with a flux ratio of $\Delta K = 2.0$. In both cases the angular diameters of the component stars are unresolved.

ity of the source. For a binary star, the visibility is a periodic function given by:

$$V^2_{\rm bin} = \frac{V_1^2 + f^2 V_2^2 + 2f|V_1||V_2|\cos\left(2\pi(u\Delta\alpha + v\Delta\beta)\right)}{(1+f)^2} \tag{1}$$

where $(\Delta\alpha, \Delta\beta)$ represent the separation of the binary in right ascension and declination, (u, v) are the spatial frequencies of the interferometer baseline projected on the sky, f is the binary flux ratio, and V_1 and V_2 are the uniform disk visibilities of the component stars (e.g. Boden 1999). The spacing between the peaks in the visibility curve gives the separation of the binary projected along the interferometer baseline while the minimum indicates the flux ratio (see Figure 3). Additionally, for interferometers that combine the light from three or more telescopes, closure phases can also be used to determine the binary separation and flux ratio (Monnier 2007). The Keck Interferometer was used to spatially resolve the orbits of three PMS double-lined spectroscopic binaries: HD 98800 B (Boden et al. 2005), V773 Tau A (Boden et al. 2007), and Haro 1-14c (Schaefer et al. 2008).

3. Prospects for the Future

Table 1 provides a summary of known double-lined and single-lined spectroscopic binaries in nearby star forming regions (Taurus-Auriga, Orion, Ophiuchus, Scorpius-

Centaurus, Lupus, TW Hydra, NGC 2264). Additional binary candidates, including some with longer periods ($P > 100$ days), are identified in Melo (2003), Guenther et al. (2007), Prato (2007), and Tobin et al. (2009). In Figure 4, I use the sample of binaries in Table 1 to plot the projected semi-major axis in angular units versus the K-band magnitude. This plot shows a lack of known PMS spectroscopic binaries at long periods (large separations) and faint magnitudes ($K > 10$ mag). As the sensitivity of long-baseline interferometers improve, it will be useful to fill in this region of parameter space. In addition to spectroscopic surveys, Gordon et al. discussed at this conference the feasibility of an interferometric survey to search for PMS binary stars.

The horizontal lines in Figure 4 show the angular resolution of 100-300 meter interferometric baselines operating at the K, H, or R-bands. Typical limiting magnitudes for the CHARA array (30-330 meter baselines) are $V \sim 10$ mag for tip/tilt guiding and $K \sim 7$ mag for fringe tracking. This is right at the edge of the distribution of PMS binaries; a few of the fainter targets might be accessible in favorable seeing conditions. With upgrades to improve the tip/tilt system and plans to add full adaptive optics to the CHARA telescopes, expected limits of $V \sim 16$ mag and $K \sim 10$ mag could bring a large portion of the known population within reach of CHARA. Likewise, the current sensitivity for the Very Large Telescope Interferometer (8-200 meter baselines) is $V \sim 13.5$ mag and $H \sim 7$ mag. The Magdalena Ridge Observatory Interferometer that is under construction (8-340 meter baselines) is expected to achieve a limiting magnitude of $H \sim 14$ mag. With combined efforts to push spectroscopic surveys for longer period binaries fainter and with the expected improvements in sensitivity of long-baseline optical/IR interferometers, we can continue assembling a large sample of low-mass PMS stars with precision masses to calibrate the evolutionary tracks.

Acknowledgments. I would like to thank M. Simon for reading through a draft of this paper.

References

Alcalá, J. M., Covino, E., Melo, C., & Sterzik, M. F. 2002, A&A, 384, 521

Alencar, S. H. P., Melo, C. H. F., Dullemond, C. P., Andersen, J., Batalha, C., Vaz, L. P. R., & Mathieu, R. D. 2003, A&A, 409, 1037

Allard, F., Hauschildt, P. H., Alexander, D. R., & Starrfield, S. 1997, ARA&A, 35, 137

Ballesteros-Paredes, J., Klessen, R. S., Mac Low, M.-M., & Vazquez-Semadeni, E. 2007, Protostars and Planets V, 63

Baraffe, I., Chabrier, G., Allard, F., & Hauschildt, P. 2003, in Brown Dwarfs, edited by E. Martín, vol. 211 of IAU Symposium, 41

Baraffe, I., Chabrier, G., Allard, F., & Hauschildt, P. H. 1998, A&A, 337, 403

Boden, A. F. 1999, in Principles of Long Baseline Interferometry, Course Notes from the 1999 Michelson Summer School, edited by P. R. Lawson (Pasadena, CA: Michelson Science Center), 9

Boden, A. F., Sargent, A. I., Akeson, R. L., Carpenter, J. M., Torres, G., Latham, D. W., Soderblom, D. R., Nelan, E., Franz, O. G., & Wasserman, L. H. 2005, ApJ, 635, 442

Boden, A. F., Torres, G., Sargent, A. I., Akeson, R. L., Carpenter, J. M., Boboltz, D. A., Massi, M., Ghez, A. M., Latham, D. W., Johnston, K. J., Menten, K. M., & Ros, E. 2007, ApJ, 670, 1214

Bonnell, I. A., Larson, R. B., & Zinnecker, H. 2007, Protostars and Planets V, 149

Cargile, P. A., Stassun, K. G., & Mathieu, R. D. 2008, ApJ, 674, 329

Chabrier, G., & Baraffe, I. 2000, ARA&A, 38, 337

Covino, E., Frasca, A., Alcalá, J. M., Paladino, R., & Sterzik, M. F. 2004, A&A, 427, 637

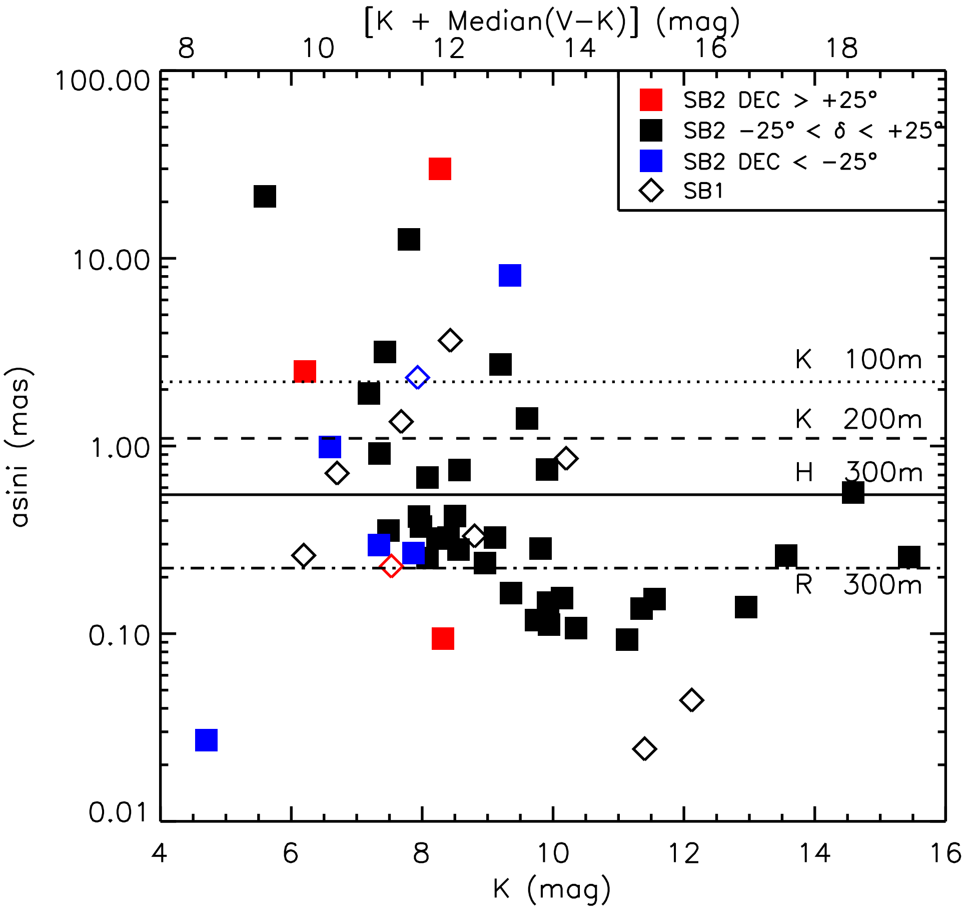

Figure 4. Distribution of projected semi-major axes of low-mass PMS spectroscopic binaries in nearby star forming regions. The semi-major axis has been scaled by the average distance to the star forming region where the star is located. The squares indicate double-lined spectroscopic binaries. Red indicates targets at northern declinations, blue southern declinations, and black declinations accessible from interferometers in both hemispheres. The open diamonds represent $a_1 \sin i$ for single-lined spectroscopic binaries. The bottom axis plots the K-band magnitude while the top axis shows a proxy for the V-band magnitude (the individual K-band magnitude of the binary plus the median $(V - K)$ for all stars plotted). The horizontal lines represent the angular resolution $(\frac{\lambda}{2B})$ for different interferometer baseline lengths and filter wavelengths (dotted: K-band, 100 m; dashed: K-band, 200 m; solid: H-band, 300 m; dash-dotted: R-band, 300 m).

Covino, E., Melo, C., Alcalá, J. M., Torres, G., Fernández, M., Frasca, A., & Paladino, R. 2001, A&A, 375, 130

D'Antona, F., & Mazzitelli, I. 1997, memsai, 68, 807

Guenther, E. W., Esposito, M., Mundt, R., Covino, E., Alcalá, J. M., Cusano, F., & Stecklum, B. 2007, A&A, 467, 1147

Guilloteau, S., & Dutrey, A. 1998, A&A, 339, 467

Hebb, L., Stempels, H. C., Aigrain, S., Collier-Cameron, A., Hodgkin, S. T., Irwin, J. M., Maxted, P. F. L., Pollacco, D., Street, R. A., Wilson, D. M., & Stassun, K. G. 2010, A&A, 522, A37+

Hillenbrand, L. A., & White, R. J. 2004, ApJ, 604, 741

Irwin, J., Aigrain, S., Hodgkin, S., Stassun, K. G., Hebb, L., Irwin, M., Moraux, E., Bouvier, J., Alapini, A., Alexander, R., Bramich, D. M., Holtzman, J., Martín, E. L., McCaughrean, M. J., Pont, F., Verrier, P. E., & Zapatero Osorio, M. R. 2007, MNRAS, 380, 541

Kenyon, S. J., & Hartmann, L. 1995, ApJS, 101, 117

Loinard, L., Torres, R. M., Mioduszewski, A. J., & Rodríguez, L. F. 2008, ApJ, 675, L29

Luhman, K. L., Stauffer, J. R., Muench, A. A., Rieke, G. H., Lada, E. A., Bouvier, J., & Lada, C. J. 2003, ApJ, 593, 1093

Mace, G. N., Prato, L., Wasserman, L. H., Schaefer, G. H., Franz, O. G., & Simon, M. 2009, AJ, 137, 3487

Marschall, L. A., & Mathieu, R. D. 1988, AJ, 96, 1956

Martín, E. L., Magazzù, A., Delfosse, X., & Mathieu, R. D. 2005, A&A, 429, 939

Mathieu, R. D. 1994, ARA&A, 32, 465

Mathieu, R. D., Adams, F. C., & Latham, D. W. 1991, AJ, 101, 2184

Mathieu, R. D., Baraffe, I., Simon, M., Stassun, K. G., & White, R. 2007, Protostars and Planets V, 411

Mathieu, R. D., Stassun, K., Basri, G., Jensen, E. L. N., Johns-Krull, C. M., Valenti, J. A., & Hartmann, L. W. 1997, AJ, 113, 1841

Mathieu, R. D., Walter, F. M., & Myers, P. C. 1989, AJ, 98, 987

Melo, C. H. F. 2003, A&A, 410, 269

Monnier, J. D. 2007, New Astronomy Reviews, 51, 604

Padgett, D. L., & Stapelfeldt, K. R. 1994, AJ, 107, 720

Palla, F., & Stahler, S. W. 1999, ApJ, 525, 772

Pasquini, L., Cutispoto, G., Gratton, R., & Mayor, M. 1991, A&A, 248, 72

Popper, D. M. 1987, ApJ, 313, L81

Prato, L. 2007, ApJ, 657, 338

Prato, L., Simon, M., Mazeh, T., McLean, I. S., Norman, D., & Zucker, S. 2002, ApJ, 569, 863

Reipurth, B., Lindgren, H., Mayor, M., Mermilliod, J.-C., & Cramer, N. 2002, AJ, 124, 2813

Reipurth, B., Lindgren, H., Nordstrom, B., & Mayor, M. 1990, A&A, 235, 197

Rosero, V., Prato, L., Wasserman, L. H., & Rodgers, B. 2011, AJ, 141, 13

Sacco, G. G., Franciosini, E., Randich, S., & Pallavicini, R. 2008, A&A, 488, 167

Schaefer, G., Prato, L., Simon, M., & Zavala, R. T. 2010, in American Astronomical Society Meeting Abstracts #215, vol. 42 of Bulletin of the American Astronomical Society, 429.25

Schaefer, G. H., Simon, M., Beck, T. L., Nelan, E., & Prato, L. 2006, AJ, 132, 2618

Schaefer, G. H., Simon, M., Prato, L., & Barman, T. 2008, AJ, 135, 1659

Siess, L., Dufour, E., & Forestini, M. 2000, A&A, 358, 593

Simon, M. 2001, in The Formation of Binary Stars, edited by H. Zinnecker & R. Mathieu, vol. 200 of IAU Symposium, 454

Simon, M., Dutrey, A., & Guilloteau, S. 2000, ApJ, 545, 1034

Stassun, K. G., Mathieu, R. D., Vaz, L. P. R., Stroud, N., & Vrba, F. J. 2004, ApJS, 151, 357

Steffen, A. T., Mathieu, R. D., Lattanzi, M. G., Latham, D. W., Mazeh, T., Prato, L., Simon, M., Zinnecker, H., & Loreggia, D. 2001, AJ, 122, 997

Stempels, H. C., & Gahm, G. F. 2004, A&A, 421, 1159

Stempels, H. C., Hebb, L., Stassun, K. G., Holtzman, J., Dunstone, N., Glowienka, L., & Frandsen, S. 2008, A&A, 481, 747

Tobin, J. J., Hartmann, L., Furesz, G., Mateo, M., & Megeath, S. T. 2009, ApJ, 697, 1103

Tomkin, J. 1983, ApJ, 271, 717

Torres, G. 2004, AJ, 127, 1187

Torres, G., Neuhäuser, R., & Guenther, E. W. 2002, AJ, 123, 1701

Torres, R. M., Loinard, L., Mioduszewski, A. J., & Rodríguez, L. F. 2009, ApJ, 698, 242

Yi, S. K., Kim, Y.-C., & Demarque, P. 2003, ApJS, 144, 259

Table 1. Sample of Spectroscopic Binaries for T Tauri Stars ($M < 1.5$ M$_\odot$)

Double-lined Spectroscopic Binaries

Name	RA (hr)	DEC (°)	SpT	V (mag)	K (mag)	P (days)	Reference
AK Sco[*]	16	−36	F5	8.8	6.6	13.6	Alencar et al. (2003)
ASAS J052821+0338.5[*]	05	+03	K1/K3	11.2	9.0	3.9	Stempels et al. (2008)
Cru 3	12	−59	K5/K5	10.8	7.5	58.3	Alcalá et al. (2002)
DQ Tau	04	+17	M0	13.7	8.0	15.8	Mathieu et al. (1997)
EK Cep[*]	21	+69	A1/G	7.9	7.6	4.4	Tomkin (1983)
GSC 06213-00306	06	−00	K1	10.9	7.4	166.9	Guenther et al. (2007)
Haro 1-14c[†]	16	−24	K5/M1.5	12.3	7.8	592.1	Schaefer et al. (2008)
HD 34700	05	+05	G0IVe	9.2	7.5	23.5	Torres (2004)
HD 98800 B[†]	11	−24	K5	9.1	5.6	314.3	Boden et al. (2005)
HD 155555	17	−66	G5	6.7	4.7	1.7	Pasquini et al. (1991)
JW 380[*]	05	−05	M5	17.2	11.1	5.3	Irwin et al. (2007)
MML 53[*]	14	−35	K2IVe	11.3	7.9	2.1	Hebb et al. (2010)
NTTS 045251+3016[†]	04	+30	K7	11.6	8.3	2525.0	Steffen et al. (2001)
NTTS 155913-2233	15	−22	K5	11.2	8.1	2.4	Prato et al. (2002)
NTTS 160905-1859	16	−18	K1	11.7	8.1	10.4	Prato et al. (2002)
NTTS 162814-2427	16	−24	K7	12.2	7.2	36.0	Mathieu et al. (1989)
Parenago 1540	05	−05	K3	11.3	7.9	33.7	Marschall & Mathieu (1988)
Parenago 1771	05	−05	K4	13.5	9.6	149.5	Prato et al. (2002)
Parenago 1802[*]	05	−05	M2	15.4	9.9	4.7	Cargile et al. (2008)
Parenago 1925	05	−05	K3	13.4	8.5	32.9	Prato et al. (2002)
Parenago 2486	05	−05	G5	11.4	9.9	5.2	Mathieu (1994)
Parenago 2494	05	−06	K0	10.8	8.4	19.5	Reipurth et al. (2002)
ROXR1 14	16	−24	M1	16.5	9.1	5.7	Rosero et al. (2011)
RX J0350.5-1355	03	−13	K0/K1	10.7	15.4	9.3	Covino et al. (2001)
RX J0441.0-0839	04	−08	G3/G8	10.4	8.6	13.6	Covino et al. (2001)
RX J0528.9+1046	05	+10	K0	10.7	10.1	7.7	Torres et al. (2002)
RX J0529.3+1210	05	+12	K7-M0	12.9	9.2	461.9	Mace et al. (2009)
RX J0529.4+0041[*]	05	+00	K1/K7	12.3	9.7	3.0	Covino et al. (2004)
RX J0530.7-0434	05	−04	K2/K2	11.5	8.6	40.5	Covino et al. (2001)
RX J0532.1-0732	05	−07	K2/K3	12.6	9.9	46.9	Covino et al. (2001)
RX J0541.4-0324	05	−03	G8/K3	11.8	9.4	5.0	Covino et al. (2001)
RX J1559.2-3814	15	−38	M1.5	13.6	9.3	474.0	Guenther et al. (2007)
RX J1622.7-2325	16	−23	M1	15.7	8.2	3.2	Rosero et al. (2011)
S29	05	−02	K9.5	14.2	11.6	8.7	Sacco et al. (2008)
S53	05	−02	M4.5	17.4	11.3	8.5	Sacco et al. (2008)
S84	05	−02	M2.5	17.8	12.9	6.1	Sacco et al. (2008)
S85	05	−02	M1.0	18.3	13.6	12.8	Sacco et al. (2008)
S89	05	−02	K2.0	16.5	14.6	13.8	Sacco et al. (2008)
UZ Tau E	04	+25	M2	11.2	7.3	19.0	Martín et al. (2005)
V1174 Ori[*]	05	−05	M0	14.3	10.3	2.6	Stassun et al. (2004)
V4046 Sgr	18	−32	K5	10.4	7.3	2.4	Stempels & Gahm (2004)
V773 Tau	04	+28	K2	10.7	6.2	51.1	Boden et al. (2007)
V826 Tau	04	+32	K7	12.1	8.3	3.9	Reipurth et al. (1990)
Walker 134	06	+09	G5	12.4	9.8	6.4	Padgett & Stapelfeldt (1994)

Single-lined Spectroscopic Binaries

Name	RA (hr)	DEC (°)	SpT	V (mag)	K (mag)	P (days)	Reference
GW Ori	05	+11	G5	9.8	6.2	241.9	Mathieu et al. (1991)
LkCa 3	04	+27	M1	12.1	7.5	12.9	Mathieu (1994)
GSC 06209-00735	06	−00	K2	11.0	8.4	2045.0	Guenther et al. (2007)
NTTS 155808-2219	15	−22	M3	13.7	8.8	16.9	Mathieu (1994)
NTTS 160814-1857	16	−18	K2	11.9	7.7	144.7	Mathieu et al. (1989)
NTTS 162819-2423S	16	−24	G8	10.6	6.7	89.1	Mathieu et al. (1989)
RX J1220.6-7539	12	−75	K2	10.7	7.9	613.9	Guenther et al. (2007)
S96	05	−02	–	15.8	12.1	3.9	Sacco et al. (2008)
VSB 111	06	+09	G8	12.4	10.2	879.0	Mathieu (1994)
VSB 126	06	+09	K0	13.4	11.4	12.9	Mathieu (1994)

[*] Eclipsing spectroscopic binary.

[†] Spatially resolved spectroscopic binary.